Review

Thermal atomic layer etching: Mechanism, materials and prospects

Chang Fang, Yanqiang Cao, Di Wu, Aidong Li*

National Laboratory of Solid State Microstructures, Department of Materials Science and Engineering, College of Engineering and Applied Sciences, Collaborative Innovation Center of Advanced Microstructures, Nanjing University, Nanjing 210093, China

ABSTRACT

In the semiconductors and related industries, the fabrication of nanostructures and nanopatterns has become progressive demand for achieving near-atomic accuracy and selectivity in etching different materials, particularly in ultra-thin gate dielectrics and ultra-thin channels used in field-effect transistors and other nanodevices below 10 nm scale. Atomic layer etching (ALE) is a novel technique for removing thin layers of material using sequential and self-limiting reactions. Different from most ALE processes using plasma-enhanced or other energetic particles-enhanced surface reactions, thermal ALE realizes isotropic atomic-level etch control based on sequential thermal-drive reaction steps that are self-terminating and self-saturating. Thermal ALE can be viewed as the reverse of atomic layer deposition (ALD), both of which define the atomic layer removal and growth steps required for advanced semiconductor fabrication. In this review, we focus on the concept and basic characteristics of the thermal ALE in comparison with ALD. Several typical thermal ALE mechanisms including fluorination and ligand-exchange, conversion-etch, oxidation and fluorination reactions are intensively introduced. The pros and cons of thermal ALE, plasma ALE, and traditional plasma etching are compared. Some representative materials and their typical thermal ALE processes are summarized. Finally, the outlook and challenges of thermal ALE are addressed.

1. Introduction

In the modern semiconductor industry, atomic-scale etching control and material selectivity are more and more important in the pattern transfer process, especially in the fabrication of nanodevices [1–3].

As is well known, reactive ion etching is the important plasma etching with directional removal and fast etching rate by using continuous processing [4]. However, plasma etching cannot meet the requirements of the current semiconductor industry precision due to process variability, plasma-induced surface damage and unlimited reactivity [5–7].

Recently, atomic layer etching has drawn great attention because of its advantages in atomic-scale etching. As the reverse process of atomic layer deposition (ALD) [8–10], the earliest report on atomic layer etching (ALE) technique can be traced back to a U.S. patent in 1988 [11]. Yoder first proposed the concept of ALE to remove a single atomic layer from the surface of synthetic diamond films, which contains four-step processes: 1. Passing NO_2 to be chemically adsorbed on diamond surface; 2. Cleaning; 3. Impulsing the diamond surface with ions of mixed precious metal and hydrogen; 4. Cleaning. Maki and Ehrlich also contributed to early ALE. In 1989, they introduced Cl_2 to form an atomic-scale passivation layer of GaAs, and then the ArF laser was used to decompose the passivation layer, obtaining self-limiting etching at the atomic level [12]. Later, Si was etched using F_2 or Cl_2 adsorption on Si and subsequent Ar^+ plasma bombardment to remove the Si surface adsorption layer with an etching rate of 0.4 Å/cycle [13]. This processing can be called plasma atomic layer etching (plasma ALE), which mainly consists of two steps: the surface adsorption process and the surface removal process. Plasma chlorination is used to adsorb chloride ions on the surface of the etched materials by chlorine-based chemistry. Removal of the surface utilizes activated ions such as neutral Ar plasma beams [14] or Cl_2 plasma [15] to bombard the surface of the materials adsorption layer, so as to achieve atomic level etching.

At the turn of the 21st century, the development of ALE was relatively slow compared to thriving ALD, because of its slow etching rate and long processing time. However, in recent years in order to reduce the size of logic components, the integration of semiconductor devices to sub-10 nm technology nodes requires urgently atomic scale controllability (< 0.5 nm) and selectivity using layer-by-layer etch processes for microelectronics industry. Traditional plasma or wet etching processes fail to meet such harsh demands in such thin-layer architectures, especially high conformality.

Recently, thermal ALE method was first reported by George's group in the University of Colorado in 2015 [16]. Unlike the anisotropic plasma ALE, the thermal ALE is etched isotropically by using thermal-drive sequential and self-limiting reactions and can be regarded as the inverse of ALD process [8–10]. The combination of ALD and ALE can define the atomic layer growth and removal required for advanced semiconductor fabrication, producing ultrasmooth thin films based on deposit/etch-back methods and conformal etching in high-aspect-ratio structures [17]. The etching accuracy reaches atomic-scale dimensions, and a large area of uniform etching surface can be obtained. At the same time, the thermal ALE can also be selectively etched according to the specific radicals or ions process. Because of the above advantages, thermal ALE is triggering tremendous research interests in searching for the most applicable etching materials, processing approach and etching mechanism.

In this review, we focus on the concept and basic characteristics of the thermal ALE in comparison with ALD. Several typical thermal ALE mechanisms including fluorination and ligand-exchange, conversion-etch, oxidation and fluorination reactions are highlighted. The advantages and disadvantages of thermal ALE, plasma ALE, and plasma etching are compared. The representative materials and their typical thermal ALE processes are summarized. This overview also discusses the prospects and challenges of thermal ALE.

2. Concept and reaction mechanisms of thermal ALE

Thermal atomic layer etching (ALE) is a technique that uses a sequence of self-limiting reactions for thin film etching. Similar to the concept of layer-by-layer growth of atomic layer deposition (ALD) [8], thermal ALE leads to the layer-by-layer removal of materials [14,18,19]. Fig. 1 shows schematics of one complete thermal ALE and ALD cycle. A typical thermal ALE cycle usually consists of two half-reactions: surface modification (half-reaction A) and surface removal (half-reaction B) in Fig. 1(a). Surface modification A refers to that a surface chemisorption layer is formed on the etched surface via precursor vapor self-limiting adsorption, similar to ALD. Surface removal B is that the surface chemisorption layer is converted to volatile etching

products by introducing proper precursor, different from ALD. Each thermal ALE cycle can also be divided into four steps, corresponding to the ALD cycle (Fig. 1(b)): (I) surface adsorption; (II) excess reactant evacuation; (III) surface removal and (IV) volatile reaction products evacuation. The I and III steps are the key surface self-limiting steps. The II and IV steps are velocity-limited evacuation steps, which depend on the residence time of reactants and products in the reaction chamber.

At the same time, according to the growth rate in ALD (growth per cycle, GPC), the etching rate (or depth) of each cycle can also be defined as EPC (etch per cycle) in thermal ALE. Due to the nature of the self-limiting reaction during thermal ALE, EPC keeps constant, which does not change with the etching process parameters when the etching process parameters such as precursor exposure time or reactant pressure attain certain critical value. Correspondingly, there is also the concept of thermal ALE window in atomic layer etching. However, ALD window is not an essential requirement. For most thermal ALE reported up to date, EPC is evidently temperature-dependent, but in few thermal ALE reactions such as removal of TiN, HfO_2 and TiO_2, ALE window has been observed [20–22].

For the thermal ALE process, it is the separated half-reaction that helps to remove the interaction between the surface modification A and the surface removal B, control the order of surface reactions, make self-limiting behavior possible, and open the thermal ALE window. That is, "discontinuity" avoids the formation of thick mixed layers and the resulting unrestricted reactivity in continuous plasma etching [23].

The chemistry of thermal ALE based on sequential fluorination and ligand-exchange reactions has been investigated firstly [17]. It can be used to etch several metal oxides, metal nitride, metal fluoride, etc. In order to broaden the choice of etched materials and types, some new strategies in thermal ALE have also been developed based on "conversion-etch" and "oxidation and fluorination reactions" mechanisms to etch SiO_2 [24], TiN [20], WO_3 and metal W [25]. Next, the representative reaction mechanisms of thermal ALE will be elaborated, respectively.
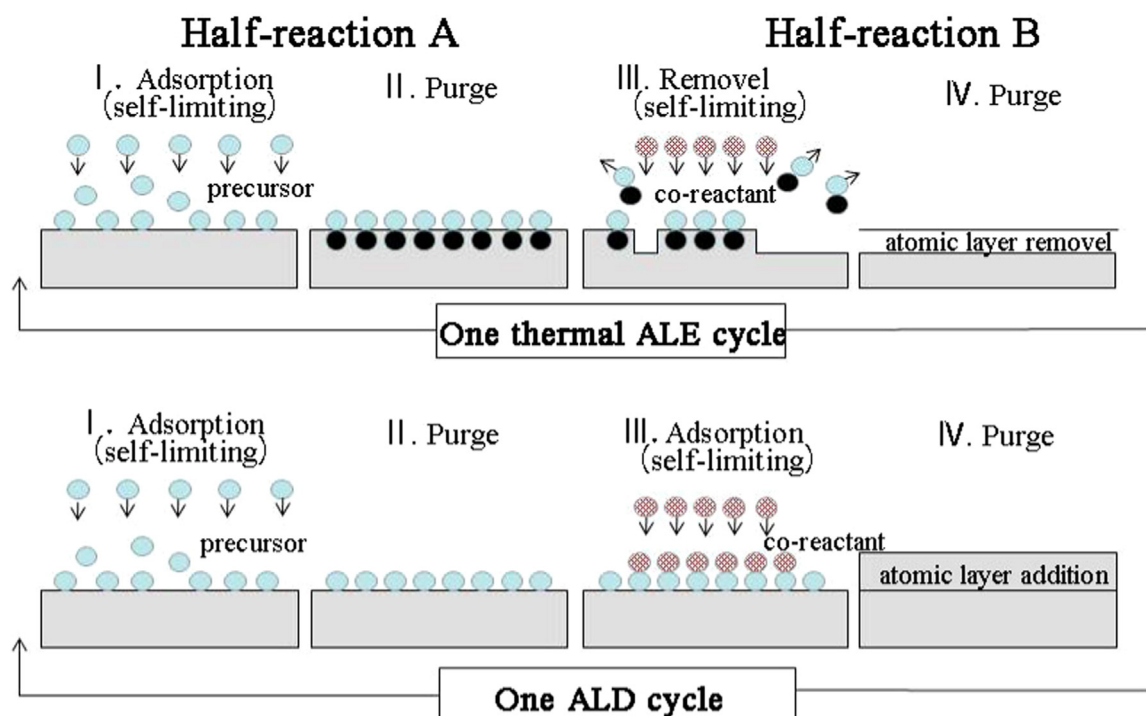

Fig. 1. Schematic illustrations of one typical cycle of (a) thermal ALE and (b) ALD.
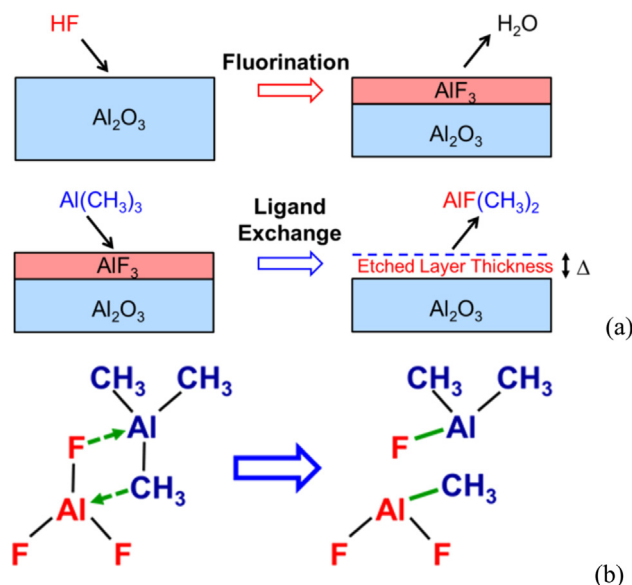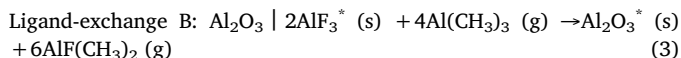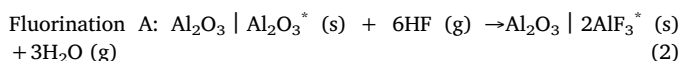
Fig. 2. Proposed reaction mechanism for thermal ALE Al_2O_3 thin films using HF and TMA as reactants. (a) Schematic of fluorination and ligand-exchange reactions during thermal ALE; (b) Schematic of the four-center ring transition state in the ligand-exchange reaction. Reproduced from Ref. [26].
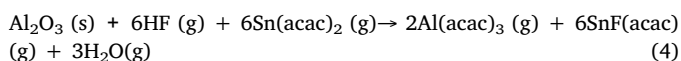
2.1. Fluorination and ligand-exchange reactions

Fig. 2 shows the proposed reaction mechanism for thermal ALE Al_2O_3 thin films using HF and trimethylaluminum ($Al(CH_3)_3$, TMA) as reactants [26]. Al_2O_3 thermal ALE is achieved by sequential, self-limiting reactions of fluorination and ligand-exchange using an AB exposure sequence. The overall reaction can be expressed as [26]:
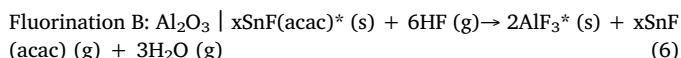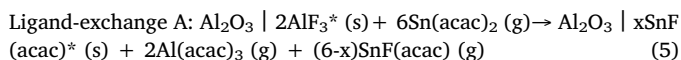
$$Al_2O_3 \text{ (s)} + 6HF(g) + 4Al(CH_3)_3 \text{ (g)} \rightarrow 6AlF(CH_3)_2 \text{ (g)} + 3H_2O \text{ (g)} \quad (1)$$
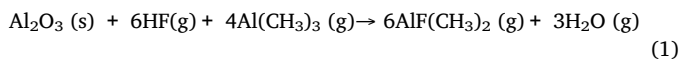
This overall reaction can be divided into two half-reaction A and B:

Fluorination A: $Al_2O_3 | Al_2O_3^* \text{ (s)} + 6HF \text{ (g)} \rightarrow Al_2O_3 | 2AlF_3^* \text{ (s)} + 3H_2O \text{ (g)}$ \quad (2)

Ligand-exchange B: $Al_2O_3 | 2AlF_3^* \text{ (s)} + 4Al(CH_3)_3 \text{ (g)} \rightarrow Al_2O_3^* \text{ (s)} + 6AlF(CH_3)_2 \text{ (g)}$ \quad (3)

The tin (II) acetylacetonate ($Sn(acac)_2$) and HF instead of TMA and HF can also be used for thermal ALE Al_2O_3 films at temperatures from 150 to 250 °C [16]. The etched surface becomes very smooth with surface roughness of only 2–3 Å (original RMS (root-mean-square) value of ~ 5 Å). The schematic for the proposed surface chemistry of thermal ALE Al_2O_3 is displayed in Fig. 3 [16]. The overall reaction can be written as [16]:

$$Al_2O_3 \text{ (s)} + 6HF \text{ (g)} + 6Sn(acac)_2 \text{ (g)} \rightarrow 2Al(acac)_3 \text{ (g)} + 6SnF(acac) \text{ (g)} + 3H_2O(g) \quad (4)$$

This overall reaction can be separated into $Sn(acac)_2$ and HF reactions:

Ligand-exchange A: $Al_2O_3 | 2AlF_3^* \text{ (s)} + 6Sn(acac)_2 \text{ (g)} \rightarrow Al_2O_3 | xSnF(acac)^* \text{ (s)} + 2Al(acac)_3 \text{ (g)} + (6\text{-}x)SnF(acac) \text{ (g)}$ \quad (5)

Fluorination B: $Al_2O_3 | xSnF(acac)^* \text{ (s)} + 6HF \text{ (g)} \rightarrow 2AlF_3^* \text{ (s)} + xSnF(acac) \text{ (g)} + 3H_2O \text{ (g)}$ \quad (6)

Whether TMA/HF or $Sn(acac)_2$/HF are used as the reactants, the etching process can be divided into four steps: I-fluorination, HF reactant is transferred into the reactor and reacts with Al_2O_3 surface to form AlF_3; II-purge, inert purge gas is introduced to remove excess HF and gaseous by-products such as H_2O, CH_4 or $SnF(acac)$; III-ligand exchange, TMA or $Sn(acac)_2$ reactant is introduced and etch happens if ligand-exchange convert AlF_3 surface layer to a stable and volatile reaction product; IV-purge, excess reactant of TMA or $Sn(acac)_2$ and volatile etch products, such as $AlF(CH_3)_2$, $Al(acac)_3$, and $SnF(acac)$, are removed.

Ligand-exchange reactions during thermal ALE are related to metal-exchange transmetalation or redistribution reactions [26,27]. Fig. 2(b) shows the four-center ring transition state in the ligand-exchange reaction during ALE Al_2O_3, which is formed by adjacent metal centers of Al in TMA and Al in AlF_3 through a bridge between F ligand and CH_3 ligand [17]. Fluorine facilitates the four-center ring transition state because of its ability to form bimetallic bridges [26,28].

Fig. 4 illustrates the impact of reactant exposure time and temperature on the sample mass change during thermal ALE Al_2O_3 thin films using TMA and HF measured by a quartz crystal microbalance (QCM) [28]. At 300 °C, nearly self-limiting etching behavior is observed after 2.0 s TMA exposure when using various TMA exposure time with a 1.0 s HF pulse and constant 30 s N_2 purge pulse in Fig. 4 (I-a). The half-reaction of ligand-exchange tends to be saturated with the etched AlF_3 surface layer of $\Delta M_{TMA} = -29$ ng/cm^2 per cycle. When the TMA pulse and N_2 purge pulse is fixed at 2.0 s and 30 s, respectively, the dependence of $\triangle M_{HF}$ of HF exposure time indicates that the nearly self-limiting adsorption characteristics are confirmed after 1.0 s HF exposure due to the saturated fluorination reaction (Fig. 4 (I-b)). The AlF_3 layer with about $\Delta M_{TMA} = 13$ ng/cm^2 per cycle is formed, which passivates the underlying Al_2O_3 film.

In addition, the sample mass change vs Al_2O_3 film etching rate is significantly dependent on the reaction temperature, as seen in Fig. 4 (II-b) [28]. With increasing the temperature, the mass loss of ΔM_{TMA} in the TMA half-reaction becomes large obviously, and meanwhile the mass gain of ΔM_{HF} in the HF half-reaction also shows an increasing trend. Considering the two factors, the larger mass loss of ΔM_{TMA} in the TMA half-reaction than mass gain of ΔM_{HF} in the HF half-reaction correspondingly leads to the increase of the etching rate with temperature. The etch rate of Al_2O_3 is 0.14 Å/cycle at 250 °C, 0.51 Å/cycle at 300 °C, and 0.75 Å/cycle at 325 °C, respectively. These data reveal that only 19% of AlF_3 is removed at 250 °C and about 75% of AlF_3 is etched at 325 °C. At different temperatures, the etching depth is linear with the number of ALE cycles.

At present, besides Al_2O_3, HfO_2, ZrO_2, AlN, and AlF_3 have been successfully etched using fluorination and ligand-exchange reactions [21,29–31]. Most thermal ALE processes are strongly temperature-dependent, except HfO_2 ALE with an ALE window ranging from 200 °C to 250 °C [21]. Selectivity in thermal ALE of Al_2O_3, HfO_2, ZrO_2, SiO_2, Si_3N_4 and TiN based on fluorination and ligand-exchange reactions has been confirmed using $Sn(acac)_2$, TMA, $Al(CH_3)_2Cl$, and $SiCl_4$ as the metal precursors and HF-pyridine as the fluorination agent, as illustrated in Fig. 5 [29]. HfO_2 can be etched by all of the metal precursors. Al_2O_3 and ZrO_2 can be etched by all of the metal precursors except $SiCl_4$ and TMA. On the contrary, SiO_2, Si_3N_4, and TiN cannot be etched by any of the metal precursors. Selective etching is related to the stability and volatility of possible reaction products. For example, SiO_2 and Si_3N_4 cannot be etched by this process because on one hand neither SiO_2 nor Si_3N_4 is etched spontaneously by HF in absence of H_2O [29,32], on the other hand the Si-F bond is too strong to undergo an effective ligand exchange reaction to generate Si-containing volatiles [30]. The negligible etching of TiN is ascribed to either the absence of stable or volatile Ti (III) reaction products or the difficulty of fluorinating Ti (IV) surface species using HF [29].

Therefore, on the basis of fluorination and ligand-exchange reactions, George's group has extended the new etching mechanisms of "conversion-etch" such as "conversion-fluorination" and "oxidation-conversion-fluorination" so as to etch more materials such as SiO_2 [24], ZnO [33], WO_3 and W [25] by thermal ALE. It will be addressed in next section.
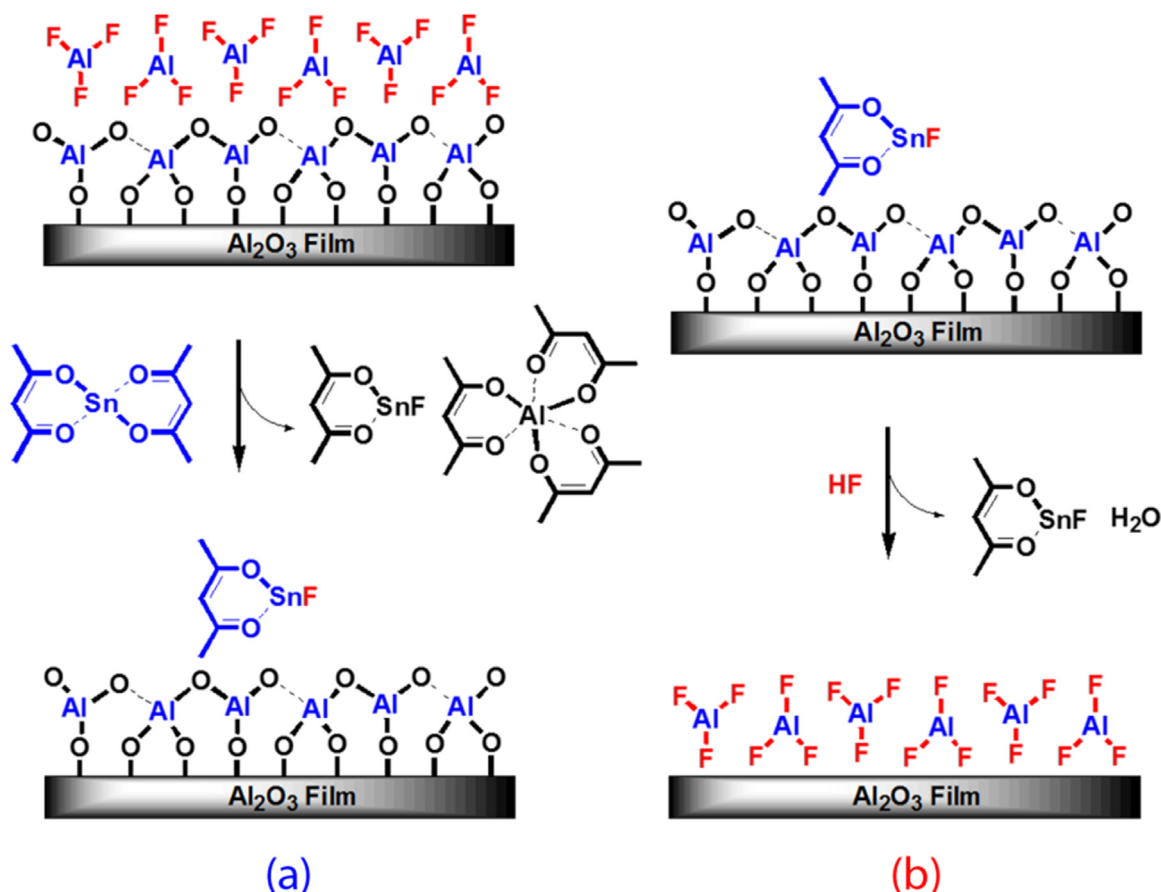
Fig. 3. Schematic of proposed reaction mechanism for Al$_2$O$_3$ thermal ALE showing (a) Sn(acac)$_2$ reaction and (b) HF reaction. Reproduced from Ref. [16].
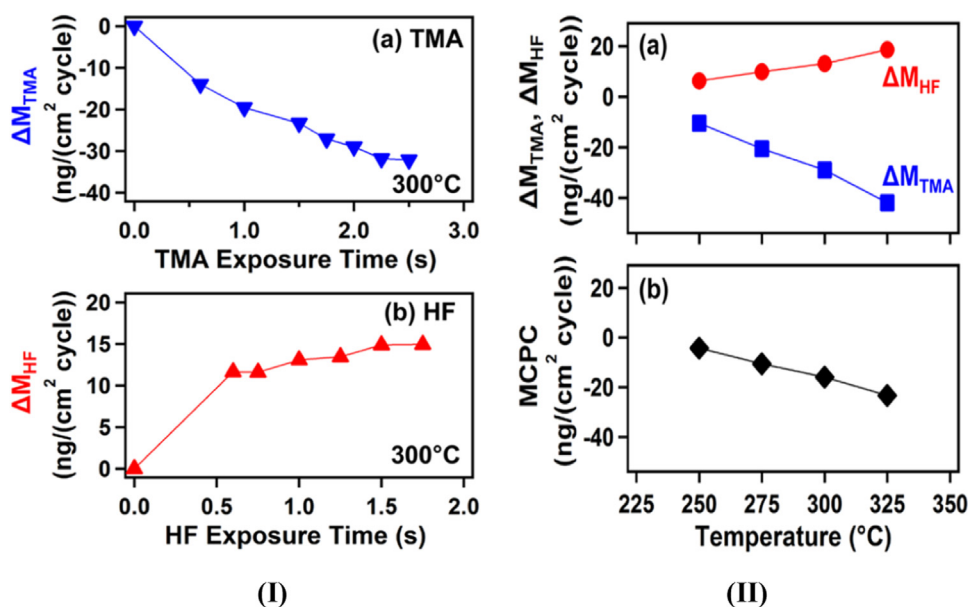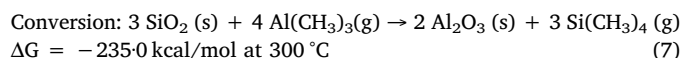

Fig. 4. Influence of reactant exposure time and temperature on the sample mass changes during thermal ALE Al$_2$O$_3$ films using TMA and HF. (I): effect of TMA (a) and HF (b) exposure time on mass changes ($\triangle$M$_{TMA}$ and $\triangle$M$_{HF}$) at 300 °C, respectively; (II): effect of temperature on $\triangle$M$_{TMA}$ and $\triangle$M$_{HF}$ of TMA, HF half-reaction (a) and mass change per ALE cycle (MCPC). Reproduced from Ref. [28].

2.2. Conversion-etch

As mentioned above, SiO$_2$ cannot be etched by fluorination and ligand exchange reactions using TMA and HF reactants at 300 °C with lower reactant pressure of 0.08 Torr [29], nevertheless through the conversion-etch method, thermal ALE SiO$_2$ thin films have been realized using an AB exposure sequence of TMA and HF at 300 °C with higher precursor pressure of 0.5, 1.0, and 4.0 Torr [24]. The key

conversion step from SiO$_2$ to Al$_2$O$_3$ can be achieved by introducing TMA reactant at higher reactant pressures:

Conversion: 3 SiO$_2$ (s) + 4 Al(CH$_3$)$_3$(g) → 2 Al$_2$O$_3$ (s) + 3 Si(CH$_3$)$_4$ (g)
ΔG = $-$235·0 kcal/mol at 300 °C   (7)

Then the following process is similar to Al$_2$O$_3$ film etching in fluorination and ligand exchange [26]. The schematic of conversion-fluorination reactions of thermal ALE SiO$_2$ using TMA/HF is shown in
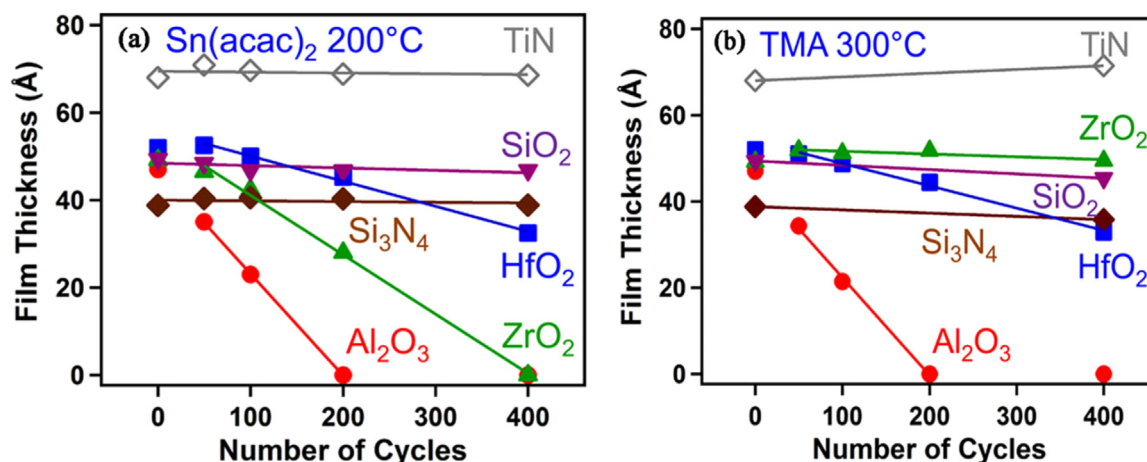
Fig. 5. Selective etching of Al_2O_3, HfO_2, ZrO_2, SiO_2, Si_3N_4, and TiN by thermal ALE using fluorination and ligand-exchange reactions: (a) $Sn(acac)_2$ at 200 °C and (b) TMA at 300 °C. Reproduced from Ref. [29].
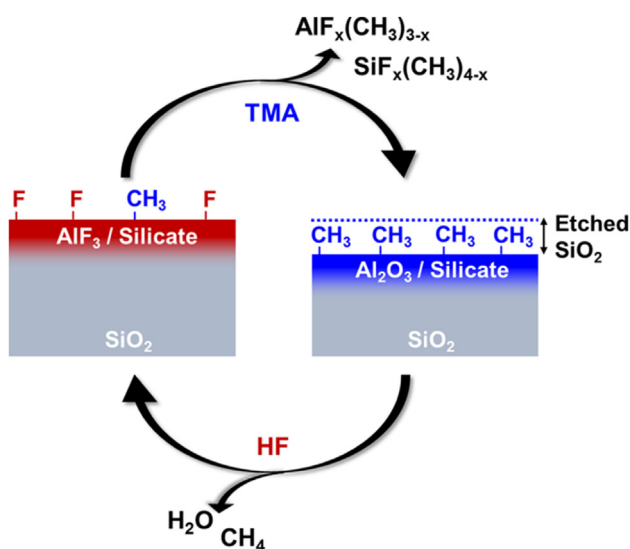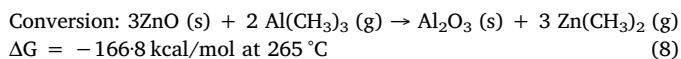

Fig. 6. Schematic of proposed reaction mechanism for TMA/HF thermal ALE SiO_2 thin films. Reproduced from Ref. [24].

Fig. 6. The conversion reaction from SiO_2 to Al_2O_3 is spontaneous because of a large negative value of ΔG. First, SiO_2 is converted to Al_2O_3/Al-silicate intermediate after TMA exposure. The following HF exposure can fluorinate Al_2O_3/Al-silicate into AlF_3 and SiO_xF_y. Subsequently, the next TMA exposure can remove AlF_3 and SiO_xF_y by a ligand exchange transmetalation reactions and then convert additional SiO_2 to Al_2O_3 again. Continuous TMA and HF reactions result in SiO_2 ALE, and each TMA/HF reaction is self-limiting behavior. The SiO_2 etching rate is dependent on static reactant pressures, such as 0.027, 0.15, 0.20, and 0.31 Å/cycle at 0.1, 0.5, 1.0, and 4.0 Torr, respectively [24]. The larger etching rates at higher reactant pressures suggest a pressure-dependent reaction mechanism for SiO_2 ALE.

Similar conversion-fluorination reactions can be observed in thermal ALE of ZnO thin films utilizing TMA and HF [33], as shown in Fig. 7. The conversion reaction (Eq. (8)) from ZnO to Al_2O_3 is also spontaneous by TMA treatment. The EPC (etch per cycle) is temperature-dependent with 2.11 Å/cycle at 265 °C, which is much higher than thermal ALE of other oxide materials such as Al_2O_3, SiO_2, HfO_2, and ZrO_2. And the etched surface becomes smooth with the decreased RMS value from 11 Å to 5.8 Å.

Conversion: $3ZnO\ (s) + 2\ Al(CH_3)_3\ (g) \rightarrow Al_2O_3\ (s) + 3\ Zn(CH_3)_2\ (g)$

$\Delta G = -166 \cdot 8\ kcal/mol\ at\ 265\ °C$ (8)

Above all, in the conversion-etch procedure, the etched surface layer is converted to a different material such as Al_2O_3 by TMA. Al_2O_3 can easily be fluorinated by HF and removed by ligand-exchange. Therefore, conversion-etch approaches may provide alternative pathways for etching additional materials with volatile fluorides using thermal ALE.

For example, such conversion-fluorination reactions can also be expected in thermal ALE SnO_2, In_2O_3 and Si_3N_4 using TMA and HF, because the TMA reactant converts them into more stable Al_2O_3 or AlN and volatile organometallic compounds such as $Sn(CH_3)_2$, $In(CH_3)_3$, and $Si(CH_3)_4$ with thermochemically favorable ΔG values [24]. Al_2O_3 can easily be etched by a variety of fluorine precursors, such as HF and SF_4, and metal precursors, such as $Sn(acac)_2$ and TMA [16,26,29]. AlN can be etched using sequential HF and $Sn(acac)_2$ exposures [30]. Therefore, the conversion-etch mechanism may be very useful in thermal ALE.

Apart from TMA, BCl_3 can also be used in conversion reactions as the reactant. BCl_3 can turn many metal oxides into B_2O_3, which easily forms volatile BF_3 and H_2O after HF exposures. WO_3 cannot be etched by fluorination and ligand-exchange reactions due to the formation of volatile fluorides causing spontaneous etching, but it could be successfully etched using an AB exposure sequence with BCl_3 and HF as the reactants via thermal ALE [25]. The conversion reaction from WO_3 to B_2O_3 with BCl_3 is thermodynamically favorable with $\Delta G°$ of $-7.8\ kcal/mol$ at 200 °C, producing volatile WO_2Cl_2. B_2O_3 layer on WO_3 surface is formed to impede further reaction of BCl_3 and WO_3, indicating the self-limiting behavior. Then B_2O_3 is spontaneously fluorinated and removed with HF to generate volatile BF_3 and H_2O, while the underlying WO_3 films act as an etch stop because HF does not react with WO_3 based on their positive standard free energy change ($\Delta G°$).

Parsons's group reported the self-limiting thermal ALE of TiO_2 using WF_6 and BCl_3 based on similar and more complicated conversion-fluorination reactions at low temperature [22], a higher EPC of ~0.6 Å/cycle at 170 °C was achieved, twice GPC of ALD TiO_2. Moreover this ALE process is evidently selective for etching TiO_2 over Al_2O_3.

The above "conversion-fluorination" mechanism of thermal ALE WO_3 using BCl_3 and HF reactants can be further extended to "oxidation-conversion-fluorination" mechanism for etching metal W using O_2/O_3, BCl_3 and HF, as presented in Fig. 8 [25]. The main difference between "conversion-fluorination" using AB cycle mode and "oxidation-conversion-fluorination" using ABC cycle mode lies in the introduction of oxygen or ozone, which oxidizes the metal W surface to a WO_3 layer. Then WO_3 layer is etched by BCl_3 and HF with similar reaction procedure. The EPC of WO_3 is temperature-dependent with 0.55 Å/cycle at 128 °C and 4.19 Å/cycle at 207 °C, while the EPC of W is ~2.5 Å/cycle at 207 °C [25]. The residual WO_3 layer (~20 Å) after thermal ALE W
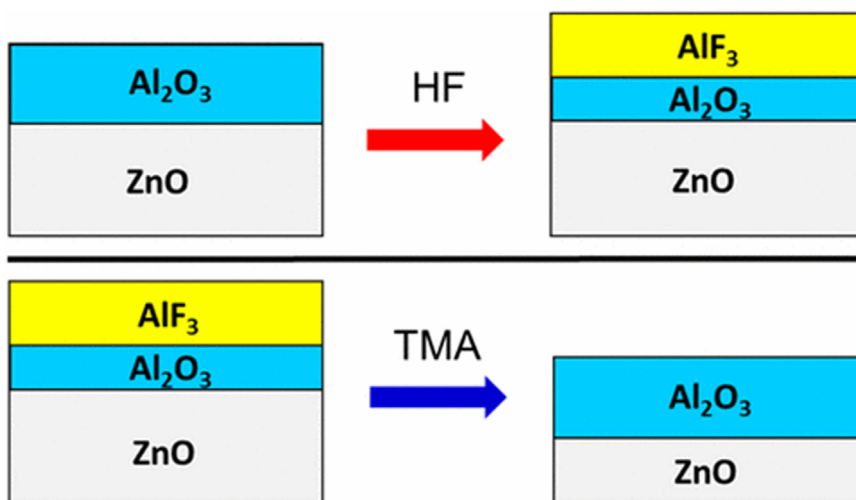
Fig. 7. Schematic of proposed reaction mechanism for HF/TMA thermal ALE ZnO thin film. Reproduced from Ref. [33].

can be removed with BCl_3 and HF without influence on the metal W layer.

Besides WO_3, the conversion-fluorination reactions using BCl_3 and HF can be employed to etch many metal oxides such as MoO_3, VO_2, V_2O_5, Ta_2O_5, GeO_2, As_2O_3, Sb_2O_3, Fe_2O_3, SnO_2, HfO_2, ZrO_2 and NbO_2 [25]. They can be converted to B_2O_3 by BCl_3 and possess volatile metal chlorides and metal oxychlorides. Moreover, in addition to metal W, the oxidation-conversion-fluorination reactions using O_2/O_3, BCl_3 and HF can also be applied to etch some metal materials such as Ta, Nb, V, W, Mo, and Cr. Overall, the conversion-etch including "conversion-fluorination" and "oxidation-conversion-fluorination" will be especially useful to enable ALE pathways for metals and metal oxides that have volatile metal fluorides and oxychlorides.

2.3. Oxidation and fluorination

In this section, we will focus on another valuable thermal ALE mechanism based on sequential, self-limiting oxidation and fluorination reactions. Fig. 9 displays the schematic of TiN ALE using O_3 and HF as
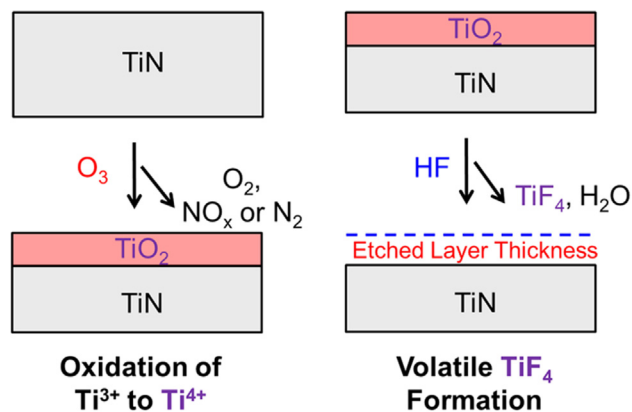

Fig. 9. Schematic for TiN ALE using O_3 and HF as the reactants. Reproduced from Ref. [20].
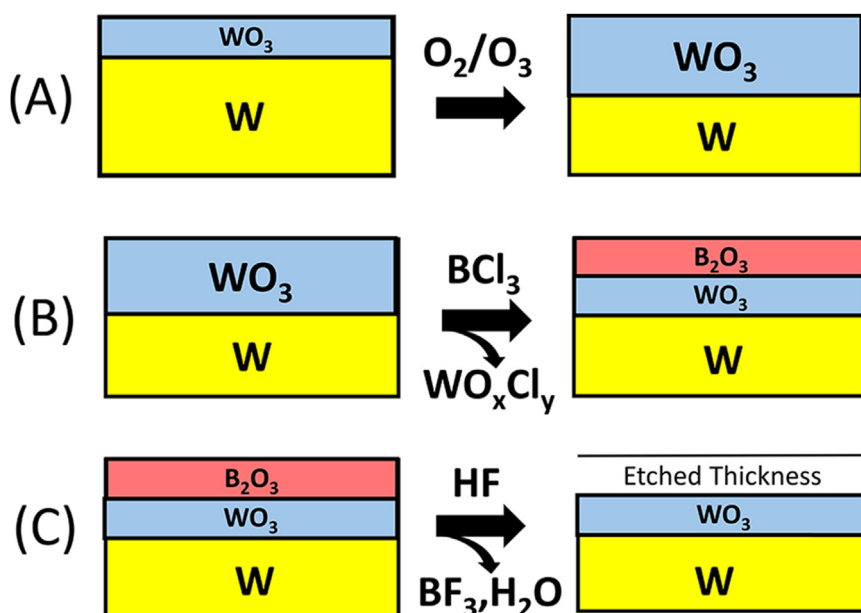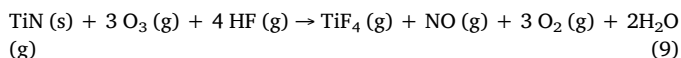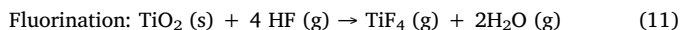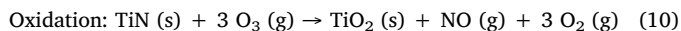

Fig. 8. Schematic of proposed reaction mechanism for thermal ALE W thin film using using O_2/O_3, BCl_3 and HF: (a) oxidation of W using O_2/O_3, (b) conversion of WO_3 to B_2O_3 using BCl_3 with volatile WO_xCl_y, and (c) fluorination of B_2O_3 by HF to form volatile BF_3 and H_2O. Reproduced from Ref. [25].

the reactants [20].

The overall etching reaction can be expressed as:

TiN (s) + 3 O_3 (g) + 4 HF (g) → TiF_4 (g) + NO (g) + 3 O_2 (g) + 2H_2O (g)   (9)

This overall reaction can be separated into O_3 and HF reactions:

Oxidation: TiN (s) + 3 O_3 (g) → TiO_2 (s) + NO (g) + 3 O_2 (g)   (10)

Fluorination: TiO_2 (s) + 4 HF (g) → TiF_4 (g) + 2H_2O (g)   (11)

In the proposed reaction mechanism, the strong oxidant (O_3) oxidizes TiN from Ti^{+3} to Ti^{+4} and forms a stable and self-passivation TiO_2 layer on the TiN substrate, which is thermodynamically favorable [20]. Herein, TiO_2 layer as a diffusion barrier prevents further oxidation, showing a self-limiting oxidation reaction. The standard free energy change $\Delta G°$ values for the HF reaction with TiO_2 is − 6.1 kcal/mol at room temperature, however it becomes positive ($\Delta G°$ = +6.1 kcal/mol) at 250 °C due to the entropic reason, indicating thermodynamically unfavorable [20]. In fact, under nonstandard conditions, the ΔG value for fluorination reaction may be negative and the etching could be continued in excess of HF vapor because the products of TiF_4 and H_2O are rapidly evacuated by N_2 purge gas. The EPC of ALE TiN increases from 0.06 Å/cycle at 150 °C to 0.20 Å/cycle at 250 °C, which confirms the speculation. Moreover, there exists ALE window for TiN ALE between 250 °C and 350 °C with nearly constant EPC value [20]. In addition, H_2O_2 can also be used as oxidation reactant to etch TiN, leading to similar surface smoothing after thermal ALE.

The selective etching of TiN is observed using O_3 and HF as the reactants in the presence of other surrounding materials, including Al_2O_3, HfO_2, ZrO_2, SiO_2, and Si_3N_4, as seen in Fig. 10 [20]. Al_2O_3, HfO_2, ZrO_2, SiO_2, and Si_3N_4 show negligible thickness change, indicating that they cannot be etched because their fluorides are stable and nonvolatile such as AlF_3, HfF_4, and ZrF_4, or their fluorides cannot be obtained in dry HF such as SiO_2, and Si_3N_4.

Similarly, two-step thermal ALE of W has been demonstrated based on sequential, self-limiting oxidation and fluorination reactions using O_2/O_3 and WF_6 as the reactants [34].

This etching reaction can be divided into O_2 and WF_6 reactions:

Oxidation: W (s) + 1·5 O_2 (g) → WO_3 (s)   (12)

Fluorination: WO_3 (s) + 0.5 WF_6 (g) → 1·5 WO_2F_2 (g)   (13)
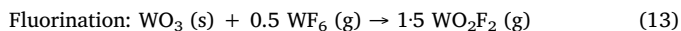
The O_2/WF_6 process is strongly temperature dependent. The EPC is only 0.34 Å/cycle at 220 °C but increases to ~6.3 Å/cycle at 300 °C,

Fig. 10. Selective etching of TiN at 250 °C using O_3 and HF in the presence of other surrounding materials of Al_2O_3, HfO_2, ZrO_2, SiO_2, and Si_3N_4. Reproduced from Ref. [20].

which is attributed to the limited volatility of the WO_2F_2 etch product at temperatures < 275 °C [34].

This thermal ALE using oxidation and fluorination mechanism should also be applicable to metal carbides, metal sulfides, metal selenides, and elemental metals that have volatile metal fluorides and oxyfluorides, which expands the number of materials that can be etched by thermal ALE methods.

Table 1 summarizes several typical thermal ALE mechanisms, reactants, etched materials and requirements. These mechanisms are valuable to clarify the understanding of ALE reactions and expand the base of available ALE processes for advanced material processing. It is expected that the multiple pathways for selective thermal ALE can be achieved by choosing proper metal precursors with various ligands and appropriate processing temperatures.

3. Basic characteristics of thermal ALE

Table 2 summaries the advantages and disadvantages of thermal ALE in comparison with plasma ALE and traditional plasma etching processes.

Herein the plasma etching mainly refers to traditional dry reactive ion etching, which continuously uses chemically reactive plasma to remove the films on wafer surface. It has the advantages of fast etching rate, high throughput, anisotropic etch capability, and wide processing temperature range. However, the principal problem is that continuous plasma etching cannot meet the increasing demands of microelectronics industry on processing accuracy of nanodevices. At present, the technology node of semiconductor processing has approached the critical scale of 10 nm, and the requirements of precision control are less than 0.5 nm. No matter what thermal ALE or plasma ALE has sequential, self-limiting reaction characteristics, they enable the possible applications in atomic-scale etching with high precision. Moreover thermal ALE can avoid the surface lattice damage and charge defects caused by plasma etching with energetic ions, thereby enhancing the reliability of nanodevices.

4. Etched materials by thermal ALE

Table 3 summarizes the typical thermal ALE processes of some representative materials, mainly involving the fluorination and ligand-exchange, conversion-etch, and oxidation and fluorination mechanisms with sequential and self-limiting behavior. Since thermal ALE processing appeared in 2015, at present some etching experiments mainly concentrate on oxides, including Al_2O_3, HfO_2, ZrO_2, ZnO, TiO_2, SiO_2, WO_3 et al., among which thermal ALE of ZnO [33], TiO_2 [22], SiO_2 [21], and WO_3 [23] uses the conversion- fluorination reactions instead of the fluorination and ligand-exchange reactions.

W Metal is commonly applied in integrated circuits as an interconnect layer and diffusion barrier [35], so W etching processes with atomic-layer dimension are very important in micro-nano device fabrications. One AB sequence [34] and one ABC sequence [23] thermal ALE W processes have been reported based on oxidation-fluorination and oxidation-conversion-fluorination reactions, respectively. They both first convert metal W to WO_3 by oxygen or ozone. Similar processing should be applicable to elemental metals such as Mo, Ta and Nb.

TiN is also a valuable material as a gate electrode for complementary metal-oxide-semiconductor (CMOS) and a copper diffusion barrier in semiconductor devices [36]. Similarly, TiN is first oxidized to form TiO_2, and then TiO_2 is fluorinated by HF and removed as volatile TiF_4 using oxidation and fluorination reactions. Thermal ALE of AlN can be realized by fluorination and ligand-exchange using HF and Sn (acac)$_2$ [30]. It is found that adding H_2 or Ar plasma exposure after each Sn(acac)$_2$ exposure dramatically increases the AlN EPC form 0.36 Å/cycle to 1.96 or 0.66 Å/cycle. This enhancement can be ascribed to the removal or desorption of acac surface species limiting the AlN etch rate [30]. Finally, AlF_3 ALE is the first example of the thermal ALE of a
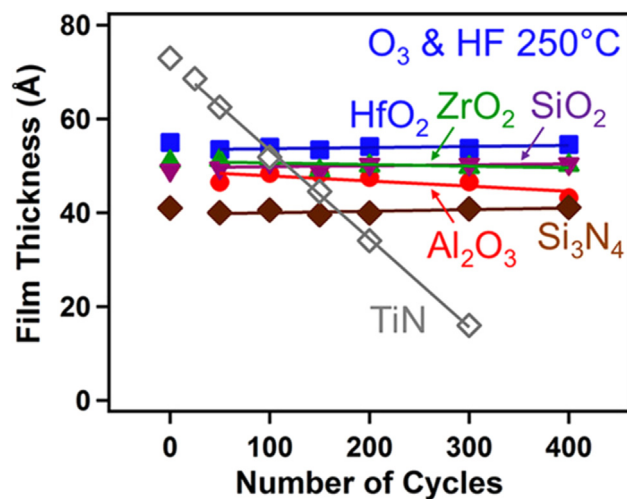
Table 1

Several typical thermal ALE mechanism, reactants, etched materials, and requirements.

Thermal ALE mechanism	Reactants	Etched materials	Requirements
Fluorination and ligand-exchange	HF/Sn(acac)$_2$ (TMA, Al(CH$_3$)$_2$Cl, SiCl$_4$)	Al$_2$O$_3$, HfO$_2$, ZrO$_2$, AlN, AlF$_3$	Stable and nonvolatile fluorides, volatile etching products in ligand-exchange
Conversion-fluorination	HF/TMA (BCl$_3$) WF$_6$/BCl$_3$	SiO$_2$, ZnO, WO$_3$, TiO$_2$	Converted to a different material such as Al$_2$O$_3$ or B$_2$O$_3$ easily be fluorinated, stable and volatile fluorides
Oxidation- conversion-fluorination	O$_2$(O$_3$)/BCl$_3$/HF	W	Metals with volatile chlorides or oxychlorides
Oxidation and fluorination	O$_2$ (H$_2$O$_2$)/HF O$_2$ (O$_3$)/WF$_6$	TiN, W	Stable and volatile metal fluorides or oxyfluorides

Table 2

Basic characteristics of thermal ALE, plasma ALE, and plasma etching processes.

	Thermal ALE	Plasma ALE	Plasma etching
Method	Discontinuous process with two half-reactions of surface adsorption and surface removal, similar to the inverse of the ALD process. By sequential, self-limiting thermal reactions, the conformal removal of sub-atomic layer is achieved.	Discontinuous process with two half-reactions of surface adsorption and surface removal. In surface removal step, plasma bombardment is used for etching. Surface adsorption step may be heat adsorption or plasma assisted adsorption.	Continuous etching process containing a reactive etching gas, plasma generates a large number of chemically active species, interacting with the material surface to form volatile products, including physical and chemical etching.
Advantage	Self-limiting, atomic layer precision, large area uniformity, conformal etching, ultra-smooth etched surfaces, ALE window, isotropic etching, selective etching	Self-limiting, low process temperature, atomic layer precision, ALE window, directional etching, selective etching	High etching rate, high throughput, low process temperature, directional etching, selective etching
Disadvantage	Low etching rate, throughput, process temperature, proper thermal ALE reaction mechanism and precursor	Low etching rate, complex plasma physics and chemistry, wafer scale uniformity	Plasma damage, etching accuracy, nonuniform, unlimited reactivity; chemical residue, complex plasma physics and chemistry
Example	Thermal ALE of Al$_2$O$_3$ films with TMA/HF, TiN with O$_2$/HF, W with O$_3$/BCl$_3$/HF	Plasma ALE of Si and W with Cl$_2$ and Ar$^+$ plasma	C$_4$F$_8$ reactive ion etching Si, CHF$_3$/O$_2$ reactive ion etching SiO$_2$

Table 3

Typical thermal ALE processes for some representative materials.

Materials	Surface adsorption	Surface removal	EPC (Å/ cycle)	Etching temperature	Ref.
Al$_2$O$_3$	HF	Sn(acac)$_2$	0.61	250 °C	[16]
	HF	TMA	0.14/0.75	250/325 °C	[26]
HfO$_2$	HF	Sn(acac)$_2$	0.117	250 °C	[21]
	HF	Al(CH$_3$)$_2$Cl	0.77	250 °C	[29]
ZrO$_2$	HF	SiCl$_4$/ Sn (acac)$_2$	0.14	350 °C/ 200 °C	[29]
	HF	Al(CH$_3$)$_2$Cl	0.117	250 °C	[29]
ZnO	HF	TMA	2.19	295 °C	[33]
TiO$_2$	WF$_6$	BCl$_3$	0.6–0.7	170 °C	[22]
SiO$_2$	HF	TMA	0.31	300 °C	[24]
WO$_3$	BCl$_3$	HF	4.19	207 °C	[25]
W	O$_3$/BCl$_3$	HF	2.5	207 °C	[25]
	O$_2$	WF$_6$	6.3	300 °C	[34]
TiN	O$_3$	HF	0.20	250 °C	[20]
AlN	HF	Sn(acac)$_2$	0.36	250 °C	[30]
	HF	Sn(acac)$_2$/H$_2$ plasma	1.96	250 °C	[30]
AlF$_3$	HF	Sn(acac)$_2$	0.069/0.63	150/250 °C	[31]

metal fluoride using Sn(acac)$_2$ and HF as reactants by yielding SnF (acac) and AlF(acac)$_2$ as volatile reaction products [31].

In summary, compared to plentiful materials prepared by ALD, now the materials etched by thermal ALE are very limited by actual verification. But it is believed that thermal ALE of more materials with atomic-scale precision will be achieved by designing feasible reaction routes and choosing proper precursors.

5. Prospects and challenges

Rapid progress is made on the atomic layer etching technology with self-limiting characteristics and atomic-scale control precision, which has great potential applications in microelectronics, optoelectronics, micro-electro-mechanical systems (MEMS) and nanotechnology fields, especially in semiconductor nanodevices. Ultra-thin gate dielectrics, ultra-thin channels, novel field-effect transistors (FET) architecture such as fin field-effect transistors (FinFET) and Gate-All-Around CMOS require near-atomic scale etching control and selectivity. Compared with the continuous plasma etching developed for more than 30 years, only atomic layer etching can meet such harsh requirements. In several material systems, thermal ALE has been confirmed to obtain controllable and conformal surface etching with sub-nanometer scale, ultra-smooth surface, no damage in high aspect-ratio structures, and possible anisotropic etching with ion or radical enhancement. As an essential counterpart to ALD, ALE and ALD can enable the atomic layer growth and removal steps for advanced semiconductor fabrication, providing new processing capabilities for constructing three-dimensional nanodevices.

Although thermal ALE has achieved exciting and promising progress recently, compared to extensive and intensive ALD research, thermal ALE is still in an early stage of development. The ALE precursor and materials have yet to be enriched greatly, and the reaction mechanism needs to be further revealed. The low etching rate, long cycling time, low throughput and high cost lead to the difficulty for transferring thermal ALE from research to manufacturing, impeding its commercial applications in industry.

When IC critical dimension and feature size shrink below 10 nm, the low etching rate of ALE becomes relatively less crucial. The quality and smoothness of etched surface and subsurface, etching fidelity in high aspect-ratio structures, and high materials selectivity become more and more important. This provides an alternative approach for thermal ALE to find the way in future semiconductor manufacturing processes. Above all, at the tipping point the development of thermal ALE is facing tremendous opportunities and challenges ahead. It is believed that emerging thermal ALE could have promising futures and prospects like ALD through continuous efforts of academia and industry.

Acknowledgments

References

[1] M. Guillorn, J. Chang, N. Fuller, J.J. Patel, Vac. Sci. Technol. B 27 (6) (2009) 2588–2592.

[2] S. Samukawa, M. Hori, S. Rauf, K. Tachibana, P. Bruggeman, G. Kroesen, J.C. Whitehead, A.B. Murphy, A.F. Gutsol, S. Starikovskaia, U. Kortshagen, J.P. Boeuf, T.J. Sommerer, M.J. Kushner, U. Czarnetzki, J. Phys. D: Appl. Phys. 45 (25) (2012) 253001.

[3] S.M. George, Chem. Rev. 110 (2010) 111–131.

[4] V.M. Donnelly, A. Kornblit, J. Vac. Sci. Technol. A 31 (5) (2013) 050825–050848.

[5] C.G.N. Lee, K.J. Kanarik, R.A. Gottscho, J. Phys. D: Appl. Phys. 47 (27) (2014) 994–1004.

[6] S. Banna, A. Agarwal, G. Cunge, M. Darnon, E. Pargon, O. Joubert, J. Vac. Sci. Technol. A 30 (4) (2012) 040801–040829.

[7] N. Marchack, J.P. Chang, J. Phys. D: Appl. Phys. 44 (17) (2011) 174011–174021.

[8] T. Faraz, F. Roozeboom, H.C.M. Knoops, W.M.M. Kessels, ECS J. Solid State Sci. Technol. 4 (6) (2015) N5023–N5032.

[9] A. Sherman, Atomic Layer Deposition For Nanotechnology: an Enabling Process for Nanotechnology Fabrication, Ivoryton Press, New York, 2008.

[10] A.D. Li, Atomic Layer Deposition Technology-Fundamental and Applications, Scientific Press, Beijing, 2016.

[11] M.N. Yoder, Atomic layer etching: U.S. Patent, 4756794A, 1988.

[12] P.A. Maki, D.J. Ehrlich, Appl. Phys. Lett. 55 (1989) 91–93.

[13] H. Sakaue, K. Asami, T. Ichihara, S. Ishizuka, K.K.Y. Horiike, Digital process for advanced VLSI's and surface reaction study, MRS Proc. (1991) 222.

[14] G.S. Oehrlein, D. Metzler, C. Li, Atomic layer etching at the tipping point: an overview, ECS J. Solid State Sci. Technol. 4 (6) (2015) N5041–N5053.

[15] C. Petit-Etienne, M. Darnon, P. Bodart, M. Fouchier, G. Cunge, E. Pargon, L. Vallier, O. Joubert, J. Vac. Sci. Technol. B 31 (1) (2013) (011201-1~8).

[16] Y. Lee, S.M. George, ACS Nano 9 (2015) 2061–2070.

[17] S.M. George, Y. Lee, ACS Nano 10 (2016) 4889–4894.

[18] C.T. Carver, J.J. Plombon, P.E. Romero, S. Suri, T.A. Tronic, R.B. Turkot, J. ECS J. Solid State Sci. Technol. 4 (2015) N5005–N5009.

[19] K.J. Kanarik, T. Lill, E.A. Hudson, S. Sriraman, S. Tan, J. Marks, V. Vahedi, R.A. Gottscho, J. Vac. Sci. Technol. A 33 (2) (2015) (20802-1~14).

[20] Y. Lee, S.M. George, Chem. Mater. 29 (2017) 8202–8210.

[21] Y. Lee, J.W. DuMont, S.M. George, ECS J. Solid State Sci. Technol. 4 (2015) N5013–N5022.

[22] C. Paul, Lemaire, N.P. Gregory, Chem. Mater. 29 (2017) 6653–6665.

[23] O. Joubert, E. Despiau-Pujo, G. Cunge, In: Proceedings of the Workshop on Atomic-Layer-Etch and Clean Technology. San Francisco, CA, 2014.

[24] J. DuMont, A.E. Marquardt, A.M. Cano, S.M. George, ACS Appl. Mater. Interfaces 9 (2017) 10296–10307.

[25] R. Nicholas, Johnson, S.M. George, ACS Appl. Mater. Interfaces 9 (2017) 34435–34447.

[26] Y. Lee, J.W. DuMont, S.M. George, Chem. Mater. 28 (2016) 2994–3003.

[27] J.C. Lockhart, Chem. Rev. 65 (1965) 131–151.

[28] H.W. Roesky, I.J. Haiduc, Chem. Soc., Dalton Trans. (1999) 2249–2264.

[29] Y. Lee, C. Huffman, S.M. George, Chem. Mater. 28 (2016) 7657–7665.

[30] N.R. Johnson, H. Sun, K. Sharma, S.M. George, J. Vac. Sci. Technol. A 34 (2016) 050603.

[31] Y. Lee, J.W. DuMont, S.M. George, J. Phys. Chem. C 119 (2015) 25385–25393.

[32] J.K. Kang, J. Chem. Phys. 116 (2002) 275–280.

[33] R. David, Zywotko, S.M. George, Chem. Mater. 29 (2017) 1183–1191.

[34] W.Y. Xie, C. Paul, Lemaire, G.N. Parsons, ACS Appl. Mater. Interfaces 10 (2018) 9147–9154.

[35] D. Choi, K. Barmak, Electron. Mater. Lett. 13 (2017) 449–456.

[36] H.J. Kim, Vac. Sci. Technol., B: Microelectron. Process. Phenom. 21 (2003) 2231–2261.